THE JOURNAL OF BIOLOGICAL CHEMISTRY VOL. 287, NO. 41, pp. 34212–34224, October 5, 2012
© 2012 by The American Society for Biochemistry and Molecular Biology, Inc. Published in the U.S.A.

KCNQ1 Channels Do Not Undergo Concerted but Sequential Gating Transitions in Both the Absence and the Presence of KCNE1 Protein*

Received for publication, March 21, 2012, and in revised form, August 3, 2010 Published, JBC Papers in Press, August 20, 2012, DOI 10.1074/jbc.M112.364901

Eshcar Meisel, Meidan Dvir, Yoni Haitin, Moshe Giladi, Asher Peretz, and Bernard Attali[1]

From the Department of Physiology and Pharmacology, the Sackler Faculty of Medicine, Tel Aviv University, Tel Aviv 69978, Israel

Background: The gating mechanisms of KCNQ1 channels are poorly understood.
Results: A thermodynamic mutant cycle analysis indicates that each subunit produces an incremental contribution to channel gating.
Conclusion: KCNQ1 channels do not undergo concerted but sequential gating transitions in both the absence and the presence of KCNE1.
Significance: Contrary to *Shaker* channels, KCNQ1 channel gating is not concerted and weakly cooperative.

The co-assembly of KCNQ1 with KCNE1 produces I_{KS}, a K^+ current, crucial for the repolarization of the cardiac action potential. Mutations in these channel subunits lead to life-threatening cardiac arrhythmias. However, very little is known about the gating mechanisms underlying KCNQ1 channel activation. *Shaker* channels have provided a powerful tool to establish the basic gating mechanisms of voltage-dependent K^+ channels, implying prior independent movement of all four voltage sensor domains (VSDs) followed by channel opening via a last concerted cooperative transition. To determine the nature of KCNQ1 channel gating, we performed a thermodynamic mutant cycle analysis by constructing a concatenated tetrameric KCNQ1 channel and by introducing separately a gain and a loss of function mutation, R231W and R243W, respectively, into the S4 helix of the VSD of one, two, three, and four subunits. The R231W mutation destabilizes channel closure and produces constitutively open channels, whereas the R243W mutation disrupts channel opening solely in the presence of KCNE1 by right-shifting the voltage dependence of activation. The linearity of the relationship between the shift in the voltage dependence of activation and the number of mutated subunits points to an independence of VSD movements, with each subunit incrementally contributing to channel gating. Contrary to *Shaker* channels, our work indicates that KCNQ1 channels do not experience a late cooperative concerted opening transition. Our data suggest that KCNQ1 channels in both the absence and the presence of KCNE1 undergo sequential gating transitions leading to channel opening even before all VSDs have moved.

The KCNQ (Kv7) subfamily of voltage-gated potassium channels (Kv)[2] comprises five members that play important functions in different tissues including heart, brain, epithelia, and inner ear (1–4). KCNQ1 can interact with either one of the five KCNE auxiliary β subunits, resulting in different channel functional characteristics (5, 6). Co-assembly of KCNQ1 with KCNE1 generates the I_{KS} potassium current, which plays a major role in the repolarization of the cardiac action potential (7, 8). Mutations in either KCNQ1 or KCNE1 genes lead to life-threatening cardiac arrhythmias such as the long QT (LQT) or short QT syndromes (3).

When expressed alone, KCNQ1 α subunits produce a delayed rectifier K^+ current that undergoes a hidden inactivation (9, 10). This inactivation is revealed by a hook of the tail current, which reflects recovery from inactivation. However, co-expression of KCNQ1 with the KCNE1 β subunit leads to a dramatic slowing of the activation kinetics, a positive shift in the voltage dependence of activation, and a suppression of inactivation (7–10). In addition, this interaction with KCNE1 also causes an increase in unitary channel conductance, leading to increased macroscopic current amplitude (11, 12). The subunit stoichiometry of KCNQ1 and KCNE1 in the I_{KS} channel complex is still debated. An assembly of two KCNE1 subunits with four KCNQ1 pore-forming subunits was suggested (13, 14), whereas other studies proposed a flexible stoichiometry of β subunits with up to four KCNE1 molecules associating with tetrameric KCNQ1 α subunits (15, 16).

Like in all voltage-gated cation channels, each KCNQ1 monomer is composed of six transmembrane segments with a voltage-sensor domain (S1-S4) and a pore domain (S5-S6). The voltage sensor domain (VSD) is endowed with charged amino acids, also called gating charges, which undergo conformational motions following alterations of the membrane electric field. The VSD provides an electromechanical coupling device that drives the opening of the channel pore. X-ray crystallographic studies of voltage-gated K^+ channels in their open state conformation have described the VSD architecture as a module of four membrane-spanning segments with the S3b helix and the charge-bearing S4 helix forming a helix-turn-helix structure, termed the paddle motif, which is buried in the membrane and moves at the protein-lipid interface (17, 18).

* This work was supported by the Deutsch-Israelische Projektkooperation (DIP) fund (Deutsche Forschungsgemeinschaft) and the Israel Science Foundation (ISF Grant 488/09).
[1] To whom correspondence should be addressed. Tel.: 972-3640-5116; Fax: 972-3640-9113; E-mail: battali@post.tau.ac.il.
[2] The abbreviations used are: Kv, voltage-gated K^+ channels; VSD, voltage sensor domain; LQT, long QT syndrome; Con′, KCNQ1 concatenated tetrameric construct.

In multisubunit channel proteins, conformational changes may give rise to cooperativity in ligand binding or voltage gating. In voltage-dependent *Shaker* K^+ channels, it is generally recognized that the independent movement of all four VSDs is followed by a last concerted cooperative transition that opens the channel (19–27). Despite numerous studies performed on *Shaker* and other Kv channels, very little is known about the putative cooperative mechanisms underlying I_{KS} channel gating. Do the voltage-induced conformational changes in the KCNQ1 tetrameric complex give rise to cooperativity in channel opening? Do they involve concerted or sequential conformational transitions in intersubunit interactions, and if so, are they affected by KCNE1? To determine the nature of subunit interactions along KCNQ1 activation gating and their modulation by KCNE1, we performed a thermodynamic mutant cycle analysis. For this purpose, we constructed a concatenated tetrameric KCNQ1 channel and introduced separately a gain of function mutation and a loss of function mutation, R231W and R243W, respectively, into the S4 helix of the VSD of one, two, three, and four subunits. Our results indicate that in both the absence and the presence of KCNE1, there is a linear relationship between the shift in the voltage dependence of activation and the number of mutated subunits, suggesting that each subunit produces an incremental contribution to channel gating. Thus, in contrast to *Shaker*-like K^+ channels, KCNQ1 channels do not undergo a late cooperative concerted opening. Instead, they experience sequential gating transitions with independent VSD movements and can open even when only one VSD assumes an activated conformation.

EXPERIMENTAL PROCEDURES

Molecular Biology—Template DNA encoding human KCNQ1 was first cloned into the pGEM vector to generate the mutant subunits. Mutations were introduced using standard PCR techniques with *Pfu* DNA polymerase. All PCR-amplified mutant products were verified by DNA sequencing. To perform the thermodynamic mutant cycle analysis, the wild-type (WT) KCNQ1 concatenated tetrameric construct (Con′) was first built into the pGEM vector, where subunits D_1, D_2, D_3, and D_4 were connected by flexible linkers (8 glycines), each harboring unique restriction sites, EcoRI, XbaI and HindIII, respectively (see Fig. 1*A*). The concatenated construct was confined by BamHI and BstEII restriction sites upstream and downstream, respectively. Using this cassette, each subunit could be removed and mutated separately by cut and paste with a pair of restriction enzymes. For example, the D_1 subunit could be cut and paste using BamHI and EcoRI restriction enzymes. WT Con′ was subsequently used as a template for constructing the various mutant subunit combinations. The Con′ was then inserted into the pcDNA3 vector to allow eukaryotic expression in CHO and HEK 293 cells.

Cell Line Culture, Cell Culture, Transfection, and Western Blot—Chinese hamster ovary (CHO) cells were maintained in Dulbecco's modified Eagle's medium (DMEM) supplemented with 2 mM glutamine, 10% fetal calf serum, and antibiotics and incubated at 37 °C in 5% $C0_2$. Cells were seeded on poly-D-lysine-coated glass coverslips in a 24-well multiwell plate and transiently transfected with Transit LT1 transfection reagent (Mirus). pIRES-CD8 was co-transfected as a surface marker. For Western blotting, HEK 293 cells were grown as CHO cells and transfected using the calcium phosphate method. Cells were washed in PBS and lysed with a buffer containing 50 mM Tris-HCl (pH 7.5), 150 mM NaCl, 0.1% Triton X-100, 1 mM EDTA, 1 mM PMSF, and a protease inhibitor mixture (1 h at 4 °C, under rotation). Cell lysates were cleared by centrifugation (10,000 × *g* for 15 min, 4 °C). Equal amounts of lysate proteins were resolved by 8% SDS-PAGE, and blots were reacted using rabbit anti-KCNQ1 antibodies (Alomone Labs).

Electrophysiology—Electrophysiological recordings were performed 40 h after transfection, using the whole-cell configuration of the patch clamp technique. Transfected cells were visualized using anti-CD8 antibody-coated beads. Data were sampled at 5 kHz and low pass-filtered at 2 kHz (Axopatch 200A amplifier with pCLAMP9 software and a four-pole Bessel low pass filter, Molecular Devices). For voltage clamp measurements, the patch pipettes were pulled from borosilicate glass (Warner Instruments Corp.) with a resistance of 3–7 megaohms and were filled with (in mM): 130 KCl, 5 Mg-ATP, 5 EGTA, 10 HEPES, pH 7.3 (adjusted with KOH), and sucrose was added to adjust osmolarity to 290 mosmol. The external solution contained (in mM): 140 NaCl, 4 KCl, 1.2 $MgCl_2$, 1.8 $CaCl_2$, 11 glucose, 5.5 HEPES, pH 7.3 (adjusted with NaOH), and sucrose was added to adjust osmolarity to 320 mosmol.

Thermodynamic Mutant Cycle Analysis—Data analysis was performed using the Clampfit program (pClamp9, Axon Instruments), Microsoft Excel, and Prism 5.0 (GraphPad). All data are expressed as mean ± S.E. Conductance (*G*) obtained from steady-state currents was calculated as $G = I/(V - V_{rev})$. *G* was then normalized to the maximal conductance. Activation curves were fit to a single Boltzmann distribution according to $G/G_{max} = 1/\{1 + \exp((V_{50} - V)/s)$, where V_{50} is the voltage at which the current is half-activated, and *s* is the slope factor. For the thermodynamic analysis, the difference in Gibbs free energy (ΔG_0) was calculated according to $\Delta G_0 = 0.2389 zFV_{50}$, where $z = RT/F_s$ (*s* is the slope factor and *R*, *T*, and *F* have their usual thermodynamic meaning). Standard errors of *z* and ΔG_0 were calculated using linear error propagation as described (52). The change in free energy difference between WT KCNQ1 and the mutant was computed by $\Delta\Delta G_0 = \Delta G_0\text{mut} - \Delta G_0\text{wt}$. High-order thermodynamic coupling analysis was performed as outlined previously (27–29). Briefly, second-order coupling free energy, reflecting coupling between two subunits, was calculated as $\Delta^2 G\,(a,b) = \Delta G_b - \Delta G_a$ according to a thermodynamic square consisting of the WT tetrameric construct, two single subunit mutants, and a double subunit mutant (see Fig. 1*A*). Third-order coupling free energy $\Delta^3 G((a,b),c)$ was calculated as the difference between the second-order coupling energies of two subunits (a,b) in the presence or absence of a third mutated subunit (c). The third-order coupling energy represents the effect of a third subunit on the interaction between two other subunits. The fourth-order intersubunit coupling free energies $\Delta^4 G(1,2)(3,4)$ reflect the energetic impact of the interaction between the (3,4) subunit pair on the intersubunit coupling free energy between the (1,2) subunit pair.

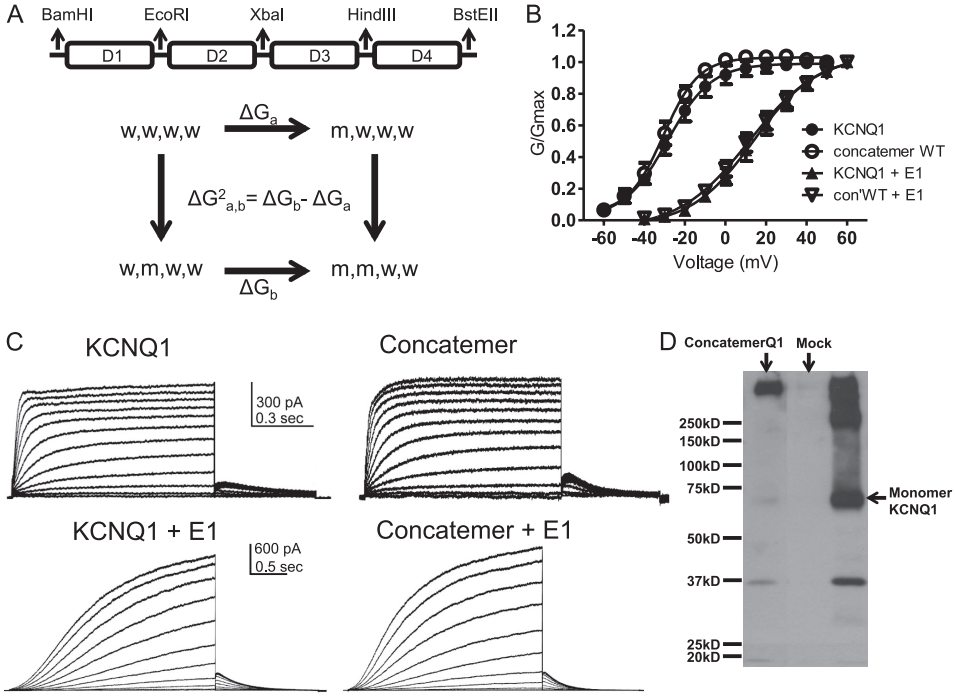

FIGURE 1. **Characterization of the KCNQ1 concatenated tetrameric construct without and with KCNE1.** *A*, *top panel*, scheme of the KCNQ1 concatenated tetrameric channel construct (Con′), where subunits D_1, D_2, D_3, and D_4 are connected by flexible linkers. Each linker (8 glycines) harbors a unique restriction site. *Bottom panel*, example of a thermodynamic mutant cycle analysis used to estimate the second-order intersubunit coupling free-energy between subunit pairs. *w* and *m* stand for wild-type and mutant subunits, respectively. *B*, conductance-voltage relations of WT monomeric and WT concatenated tetrameric KCNQ1 constructs in the absence or presence of KCNE1. Data were fit with a single Boltzmann function. *C*, representative current traces of WT monomeric and WT concatenated tetrameric KCNQ1 constructs in the absence or presence of KCNE1. CHO cells were held at −90 mV. For KCNQ1, the membrane voltage was stepped for 1 s from −60 mV to +50 mV in 10-mV increments and then repolarized for 0.5 s to −60 mV. In the presence of KCNE1, the membrane voltage was stepped for 3 s from −50 mV to +60 mV in 10-mV increments and then repolarized for 1.5 s to −60 mV. *D*, Western blot showing lysates from HEK 293-transfected empty vector (*Mock*) and KCNQ1 monomeric and concatenated tetrameric constructs.

RESULTS

Concatenated Tetrameric KCNQ1 Channels Display Similar Properties to Those of the Monomeric Construct—To perform the thermodynamic mutant cycle analysis, the WT KCNQ1 concatenated tetrameric construct (Con′) was first built into the pGEM vector, where subunits D_1, D_2, D_3, and D_4 were connected by flexible linkers (8 glycines), each harboring unique restriction sites (Fig. 1*A*). WT Con′ was subsequently used as a template for constructing the various mutant subunit combinations. WT Con′ was then inserted into the pcDNA3 vector to allow eukaryotic expression in CHO and HEK 293 cells. This strategy enabled us to cut and paste mutated subunits in any chosen combination. Concatenated tetrameric channel constructs were previously used for examining homo- and hetero-tetrameric assembly, cooperativity in intersubunit interactions, and inactivation (19, 27, 30–33). To ensure that our construct was expressed as a concatenated tetrameric channel protein, we compared its expression in HEK 293 cells with that of the monomeric KCNQ1 protein by examining its molecular mass in SDS-PAGE under reducing conditions followed by Western blotting. The monomeric KCNQ1 construct appeared as a main immunoreactive band of about 70 kDa accompanied by higher molecular mass aggregates and a minor degradation band product of about 37 kDa. In contrast, the Con′ construct expressed a major high molecular mass immunoreactive band of more than 280 kDa, roughly corresponding to the tetrameric channel protein (Fig. 1*D*). To validate the functional use of the Con′ construct, the electrophysiological properties of the WT monomeric construct and WT concatenated tetrameric KCNQ1 were compared in transfected CHO cells using the whole-cell patch clamp technique (Fig. 1, *B* and *C*). Results indicate that in both the absence and the presence of KCNE1, the WT Con′ exhibited similar kinetic properties and similar voltage dependence to those of the monomeric KCNQ1 construct (WT monomeric KCNQ1, $V_{50} = -28.6 \pm 0.5$ mV; $s = 10.8 \pm 0.4$ mV, $n = 6$; WT Con′, $V_{50} = -30.6 \pm 0.6$ mV; $s = 8.7 \pm 0.5$ mV, $n = 6$; WT monomeric KCNQ1+KCNE1, $V_{50} = 13.9 \pm 0.6$ mV; $s = 15.6 \pm 0.7$ mV, $n = 10$; WT Con′+KCNE1, $V_{50} = 11.5 \pm 0.9$ mV; $s = 17.4 \pm 1.0$ mV, $n = 12$) (Fig. 1, *B* and *C*). A similar hooked tail current that reflects recovery from inactivation was observed in the WT Con′ and the monomeric KCNQ1 construct (9, 10) (Fig. 1*C*). Thus, the concatenated tetrameric KCNQ1 channel retained the biophysical properties of the monomeric construct, thereby validating its functional use to explore subunit interactions upon channel gating.

Each KCNQ1 Subunit Endowed with a Gain of Function Mutation in the VSD Produces an Incremental Gating Perturbation—To determine the possible cooperative nature of subunit interactions involved in KCNQ1 gating and to explore whether VSD motions occur in a sequential or concerted manner in the absence and presence of KCNE1, we introduced mutations that dramatically disturb channel gating in the S4 segment of the voltage sensor and applied a thermodynamic mutant cycle analysis (Fig. 1*A*) (27–29). Two different muta-

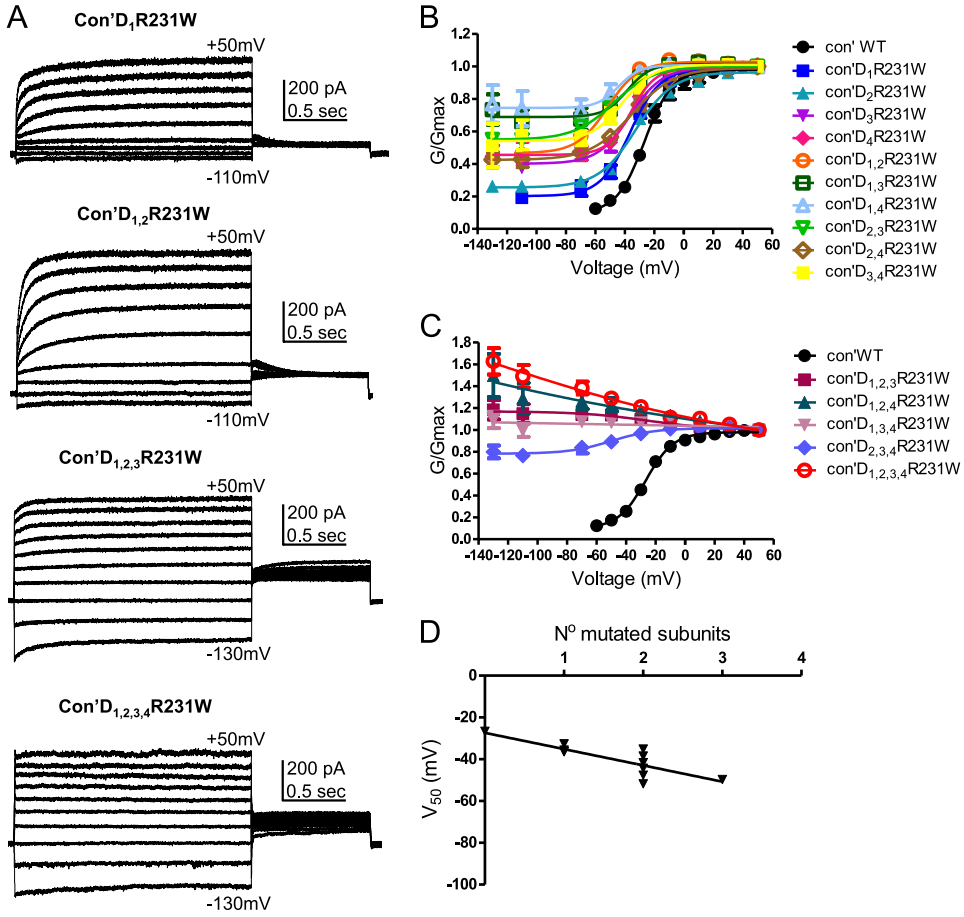

FIGURE 2. **R231W-bearing KCNQ1 subunits produce a gradual left-shift in the voltage dependence of activation.** *A*, representative current traces of Con′, with one, two, three, and four subunits harboring the R231W mutation. CHO cells were held at −90 mV. The membrane voltage was stepped for 3 s from −130 mV or −110 mV to +50 mV in 20-mV increments and then repolarized for 1.5 s to −60 mV. *B* and *C*, conductance-voltage relations of the different combinations of R231W-bearing subunits in Con′. Data were fitted with a single Boltzmann function, except for Con′$D_{1,2,3}$R231W, Con′$D_{1,2,4}$R231W, and Con′$D_{1,3,4}$R231W where connecting lines are shown. Fitting parameters are summarized in Tables 1 and 2. *D*, linear regression analysis of the different V_{50} values *versus* the number of R231W mutated subunits, $r^2 = 0.68$, $P_v = 0.0009$.

tions were made separately, a gain of function mutation and a loss of function mutation.

The gain of function mutation, R231W, was generated at the second arginine of the S4 helix. We and others previously showed that mutating this residue by tryptophan or alanine destabilizes channel closure and produces time- and voltage-independent constitutively open channels, even in the presence of KCNE1, suggesting that the loss of the positive charge at this position prevents the channel from closing and dominates the effect of KCNE1 (34–37). Interestingly, a cysteine mutation of this same residue, R231C, was shown to cause LQT1 syndrome and familial atrial fibrillation (38). When we sequentially introduced the mutation R231W into an incremental number of VSDs, we observed upon KCNQ1 expression alone three measurable effects (Fig. 2, *A–C*, Fig. 3, *A* and *B*, Table 1). (*a*) The first effect was a progressive left-shift of the voltage dependence of channel activation (V_{50}) (WT Con′, $V_{50} = -26.6 \pm 0.8$ mV, $n = 9$; Con′D_1R231W, $V_{50} = -36.4 \pm 0.9$ mV, $n = 11$; Con′$D_{1,2}$R231W, $V_{50} = -51.8 \pm 2.2$ mV, $n = 12$). (*b*) The second effect was an increased voltage-independent conductance fraction G_{min}, given by the horizontal asymptote of the Boltzmann function (WT Con′, $G_{min} = 0.098 \pm 0.021$, $n = 9$; Con′D_1R231W, $G_{min} = 0.202 \pm 0.014$, $n = 11$; Con′$D_{1,2}$R231W, $G_{min} = 0.466 \pm 0.026$, $n = 12$; Con′$D_{1,2,3}$R231W and Con′$D_{1,2,3,4}$R231W $G_{min} = 1$, $n = 12–13$; Fig. 2, *B* and *C*). Consequently, the left-shift in steady-state activation (V_{50}) was accompanied by an increased fractional constitutive conductance, G_{min}. The more negative the V_{50}, the larger the G_{min} (Fig. 3*C*). (*c*) The third effect was an increasing component of the constitutive current measured by the ratio of the instantaneous current over the steady-state current, I_{ins}/I_{ss} (Fig. 3*B*; WT Con′, $I_{ins}/I_{ss} = 0.27 \pm 0.02$; Con′$D_1$R231W, $I_{ins}/I_{ss} = 0.36 \pm 0.03$; Con′$D_{1,2}$R231W, $I_{ins}/I_{ss} = 0.48 \pm 0.04$; Con′$D_{1,2,3}$R231W, $I_{ins}/I_{ss} = 0.83 \pm 0.02$; Con′$D_{1,2,3,4}$R231W, $I_{ins}/I_{ss} = 0.99 \pm 0.01$; $n = 9–12$). With the increasing number of mutated VSDs, the KCNQ1 current progressively lost its time and voltage dependence such that it was impossible to determine the V_{50} values in the concatenated constructs bearing three and four mutated VSDs, Con′$D_{1,2,3}$R231W, Con′$D_{1,2,4}$R231W, Con′$D_{1,3,4}$R231W, and Con′$D_{1,2,3,4}$R231W (Figs. 2, *A–C*, and 3, *A* and *B*). We observed a linear relationship between the V_{50} values of the *G-V* curves and the number of mutated subunits, suggesting independence of the VSD motions (Fig. 2*D*). Some positional effect was noticed with the concatenated constructs bearing two mutated VSDs, notably the pairs where the mutation was introduced in two diagonally

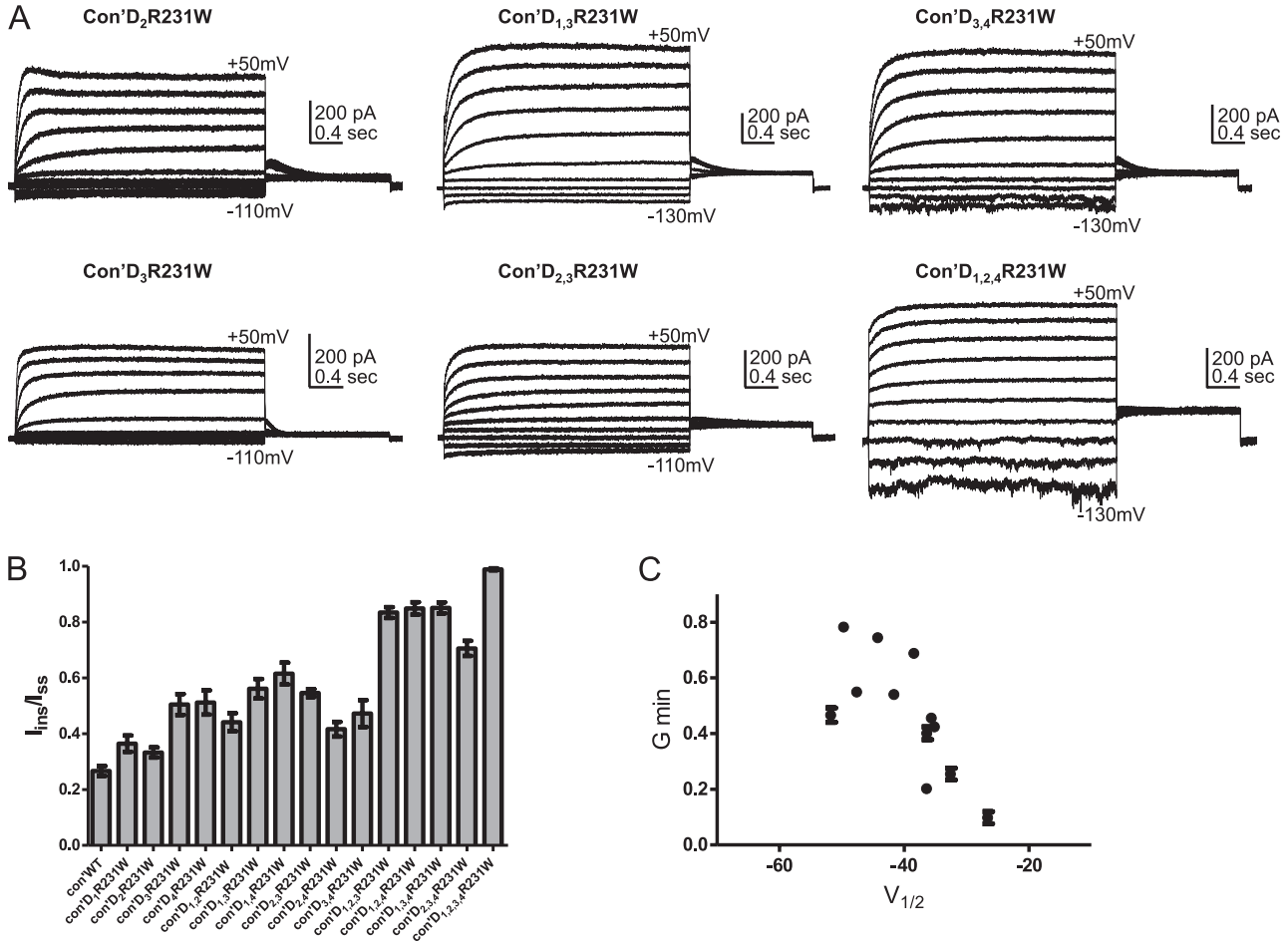

FIGURE 3. **R231W-bearing KCNQ1 subunits produce a gradual increase in the instantaneous component of the current and in the fractional constitutive conductance.** *A*, representative traces of Con′ harboring the indicated combinations of R231W mutated subunits. The membrane voltage was stepped for 3 s from −130 mV or −110 mV to +50 mV in 20-mV increments and then repolarized for 1.5 s to −60 mV. *B*, the constitutive current, I_{ins}/I_{ss}, was measured at +50 mV by the ratio of the instantaneous current over the steady-state current of the indicated combinations of subunits harboring the R231W mutation. *C*, for all Con′R231W combinations, the fractional constitutive conductances, G_{min}, given by the horizontal asymptote of the Boltzmann function, were plotted *versus* their respective V_{50} values.

TABLE 1

Gating parameters of concatenated KCNQ1 and its mutants expressed alone

V_{50} (half-activation voltage) and z (equivalent gating charge) were derived by fitting with a single Boltzmann function and are expressed as mean ± S.E. ΔG_0, $\Delta\Delta G_0$, and their standard errors were calculated as described under "Experimental Procedures." –, not detectable.

Subunits mutated	Mutation									
	R231W					R243W				
	V_{50}	z	ΔG_0	$\Delta\Delta G_0$	n	V_{50}	z	ΔG_0	$\Delta\Delta G_0$	n
	mV		*kcal/mol*	*kcal/mol*		*mV*		*kcal/mol*	*kcal/mol*	
WT	−26.6 ± 0.8	2.7 ± 0.2	−1.67 ± 0.01		9	−26.6 ± 0.8	2.7 ± 0.2	−1.67 ± 0.01		9
D_1	−36.4 ± 1.0	2.5 ± 0.2	−2.12 ± 0.01	−0.45 ± 0.02	11	−26.8 ± 0.2	2.4 ± 0.0	−1.45 ± 0.00	0.22 ± 0.01	16
D_2	−32.6 ± 2.3	2.0 ± 0.3	−1.51 ± 0.02	0.16 ± 0.02	14	−25.8 ± 0.7	2.2 ± 0.1	−1.33 ± 0.01	0.34 ± 0.01	18
D_3	−36.4 ± 2.2	2.3 ± 0.4	−1.95 ± 0.02	−0.28 ± 0.02	11	−26.7 ± 0.5	2.5 ± 0.1	−1.54 ± 0.01	0.13 ± 0.01	12
D_4	−35.7 ± 0.6	3.1 ± 0.2	−2.56 ± 0.01	−0.89 ± 0.01	12	–	–	–	–	–
$D_{1,2}$	−51.8 ± 2.2	2.5 ± 0.4	−2.93 ± 0.04	−1.26 ± 0.04	12	−26.2 ± 1.1	2.8 ± 0.3	−1.68 ± 0.01	−0.01 ± 0.01	6
$D_{1,3}$	−38.4 ± 3.2	3.3 ± 1.0	−2.90 ± 0.06	−1.23 ± 0.06	17	−27.2 ± 2.0	3.6 ± 0.9	−2.28 ± 0.04	−0.61 ± 0.04	8
$D_{1,4}$	−44.3 ± 2.3	3.5 ± 0.9	−3.57 ± 0.06	−1.9 ± 0.06	17	–	–	–	–	–
$D_{2,3}$	−47.6 ± 0.9	1.9 ± 0.1	−2.08 ± 0.01	−0.40 ± 0.01	17	−29.5 ± 1.3	3.2 ± 0.4	−2.14 ± 0.02	−0.47 ± 0.02	19
$D_{2,4}$	−35.1 ± 0.9	1.8 ± 0.1	−1.47 ± 0.01	0.20 ± 0.01	13	–	–	–	–	–
$D_{3,4}$	−41.7 ± 2.1	2.4 ± 0.4	−2.33 ± 0.03	−0.66 ± 0.03	11	–	–	–	–	–
$D_{1,2,3}$	–	–	–	–	10	−26.7 ± 2.0	3.5 ± 0.8	−2.16 ± 0.03	−0.49 ± 0.04	10
$D_{1,2,4}$	–	–	–	–	12	–	–	–	–	–
$D_{1,3,4}$	–	–	–	–	19	–	–	–	–	–
$D_{2,3,4}$	−49.7 ± 3.7	1.8 ± 0.4	−2.04 ± 0.03	−0.36 ± 0.03	13	–	–	–	–	–
$D_{1,2,3,4}$	–	–	–	–	13	−21.1 ± 2.4	3.5 ± 1.0	−1.71 ± 0.03	−0.04 ± 0.04	11

facing subunits (Con′$D_{1,3}$R231W and Con′$D_{2,4}$R231W) whose V_{50} values were more depolarized than those of adjacent mutated subunits pairs (Fig. 2*B*, Table 1). As expected, when compared with KCNQ1 alone, the co-expression of KCNE1 produced a right-shift in the voltage dependence of activation and thereby partially restored the time and voltage dependence,

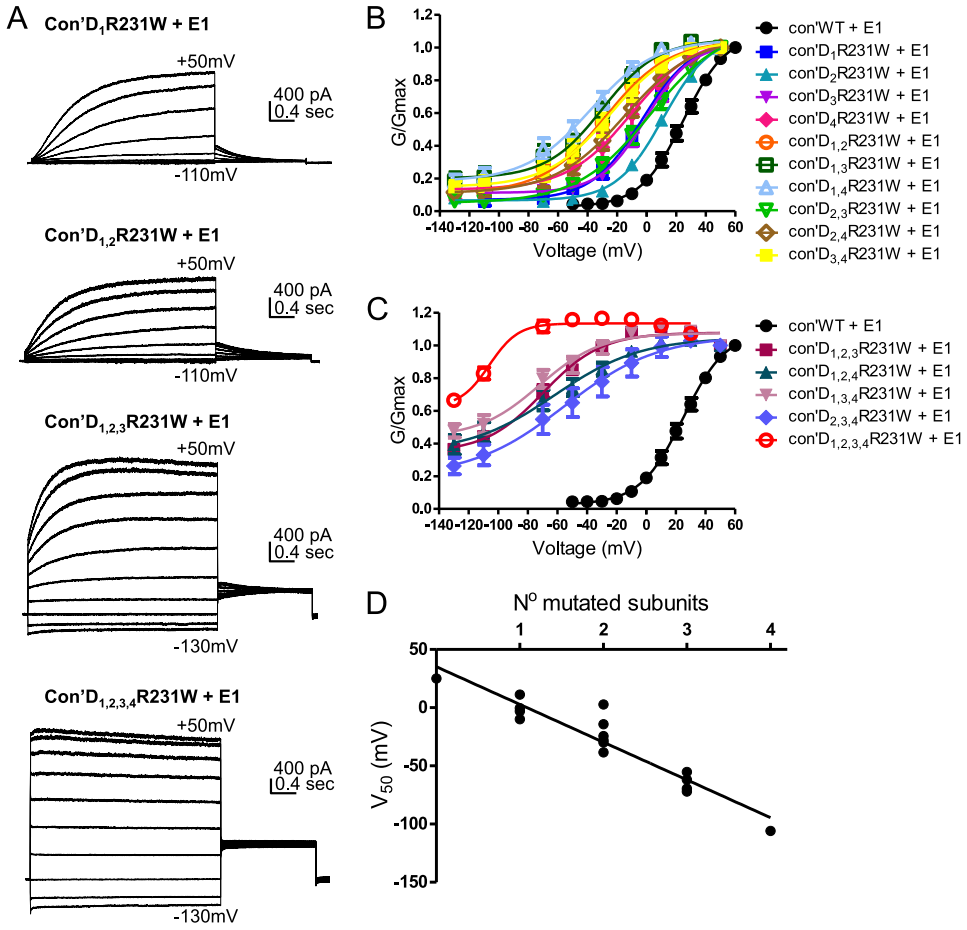

FIGURE 4. **R231W-bearing KCNQ1 subunits in the presence of KCNE1 produce a gradual left-shift in the voltage dependence of activation.** *A*, representative current traces of Con′, with one, two, three, and four subunits harboring the R231W mutation, in the presence of KCNE1. The membrane voltage was stepped for 3 s from −130 mV or −110 mV to +50 mV in 20-mV increments and then repolarized for 1.5 s to −60 mV. *B* and *C*, conductance-voltage relations of the different combinations of R231W-bearing subunits in Con′, in the presence of KCNE1. Data were fitted with a single Boltzmann function. *D*, linear regression analysis of the different V_{50} values *versus* the number of R231W mutated subunits, in the presence of KCNE1; $r^2 = 0.89$, $P_v < 0.0001$.

which was lost in the concatenated constructs bearing one, two, or three mutated VSDs such as Con′D_1R231W, Con′$D_{1,2}$R231W, and Con′$D_{1,2,3}$R231W (compare Fig. 2, *A–C*, Fig. 3, *A* and *B*, and Table 1 with Fig. 4, *A–C*, Fig. 5, *A* and *B*, and Table 2). However, KCNE1 was unable to restore the time and voltage dependence of the constitutive current generated by the concatenated construct bearing all four mutated VSDs, Con′$D_{1,2,3,4}$R231W (Fig. 4, *A* and *C*). Remarkably, KCNE1 co-expression did not change fundamentally the mechanistic features underlying KCNQ1 activation gating. With an increasing number of mutated VSDs, an incremental effect on channel gating was easily detected in the presence of KCNE1 (Figs. 4, *A–C*, and 5*A*, Table 2). A gradual left-shift of the voltage dependence of channel activation was noticed (WT Con′+KCNE1, $V_{50} = 25.0 \pm 0.6$ mV, $n = 14$; Con′D_1R231W+KCNE1, $V_{50} = -3.1 \pm 0.8$ mV, $n = 7$; Con′$D_{1,2}$R231W+KCNE1, $V_{50} = -27.9 \pm 2.8$ mV, $n = 17$; Con′$D_{1,2,3}$R231W+KCNE1, $V_{50} = -69.6 \pm 6.9$ mV, $n = 17$; Con′$D_{1,2,3,4}$R231W+KCNE1, $V_{50} = -106.0 \pm 4.8$ mV, $n = 13$). As with KCNQ1 alone, we found in the presence of KCNE1 a linear relationship between the V_{50} values and the number of mutated subunits, suggesting independence of the VSD motions even with KCNE1 (Fig. 4*D*). Similarly, a correlation was observed between the left-shift in steady-state activation (V_{50}) and the increased fractional constitutive conductance, G_{min} (Fig. 5*C*). Hence, an increasing component of the constitutive current was measured (WT Con′+KCNE1, $I_{ins}/I_{ss} = 0.03 \pm 0.01$; Con′$D_1$R231W+KCNE1, $I_{ins}/I_{ss} = 0.12 \pm 0.03$; Con′$D_{1,2}$R231W+KCNE1, $I_{ins}/I_{ss} = 0.26 \pm 0.05$; Con′$D_{1,2,3}$R231W+KCNE1, $I_{ins}/I_{ss} = 0.52 \pm 0.02$; Con′$D_{1,2,3,4}$R231W+KCNE1, $I_{ins}/I_{ss} = 0.96 \pm 0.01$; $n = 7–17$). In the presence of KCNE1, a moderate positional effect was noticed with the concatenated constructs bearing two mutated VSDs when considering the V_{50} and I_{ins}/I_{ss} values, with Con′$D_{2,3}$R231W displaying a more depolarized V_{50} and a lower constitutive current when compared with the other concatenated mutated pairs (Figs. 4*B* and 5*B*, Table 2).

So far, for the mutant R231W, the correlation between the number of mutated subunits with the left-shift in steady-state activation (V_{50}) as well as the increase in fractional constitutive conductance (G_{min}) and constitutive current (I_{ins}/I_{ss}) suggests an independence of VSD movements, with each subunit incrementally contributing to channel gating. Thus, contrary to *Shaker* channels, the data imply that KCNQ1 channels in both the absence and the presence of KCNE1 do not experience a late cooperative concerted opening but rather undergo sequential gating. However, it could be argued that these mechanistic features were observed only because the gain of function muta-

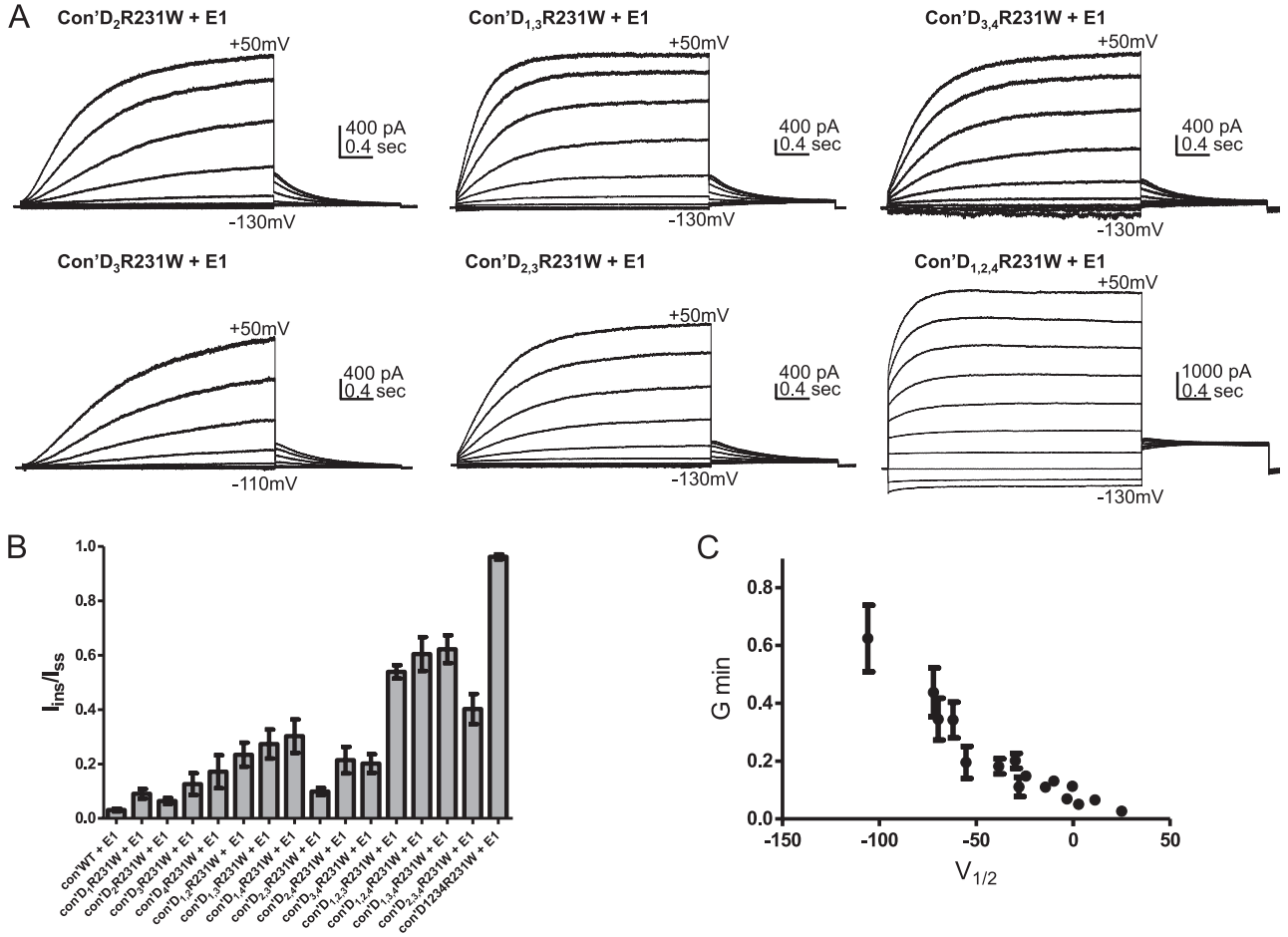

FIGURE 5. **R231W-bearing KCNQ1 subunits in the presence of KCNE1 produce a gradual increase in the instantaneous component of the current and in the fractional constitutive conductance.** *A*, representative traces of Con′ harboring the indicated combinations of R231W mutated subunits in the presence of KCNE1. The membrane voltage was stepped for 3 s from −130 mV or −110 mV to +50 mV in 20-mV increments and then repolarized for 1.5 s to −60 mV. *B*, the constitutive current, I_{ins}/I_{ss}, was measured at +50 mV by the ratio of the instantaneous current over the steady-state current of the indicated combinations of subunits harboring the R231W mutation co-expressed with KCNE1. *C*, for all Con′R231W combinations co-expressed with KCNE1, the fractional constitutive conductances, G_{min}, were plotted *versus* their respective V_{50} values.

TABLE 2

Gating parameters of concatenated KCNQ1 and its mutants expressed with KCNE1

V_{50} (half-activation voltage) and z (equivalent gating charge) were derived by fitting with a single Boltzmann function and are expressed as mean ± S.E. ΔG_0, $\Delta\Delta G_0$, and their standard errors were calculated as described under "Experimental Procedures." –, not detectable.

Subunits mutated	Mutation									
	R231W + KCNE1					R243W + KCNE1				
	V_{50}	z	ΔG_0	$\Delta\Delta G_0$	n	V_{50}	z	ΔG_0	$\Delta\Delta G_0$	n
	mV		*kcal/mol*	*kcal/mol*		*mV*		*kcal/mol*	*kcal/mol*	
WT	25.0 ± 0.6	1.8 ± 0.1	1.01 ± 0.00		14	25.0 ± 0.6	1.8 ± 0.1	1.01 ± 0.00		14
D_1	−3.1 ± 0.8	1.5 ± 0.1	−0.11 ± 0.00	−1.12 ± 0.00	7	38.6 ± 0.6	1.9 ± 0.1	1.67 ± 0.03	0.66 ± 0.03	18
D_2	11.3 ± 1.6	1.6 ± 0.1	0.42 ± 0.00	−0.59 ± 0.01	27	35 ± 0.7	1.8 ± 0.1	1.42 ± 0.03	0.40 ± 0.03	26
D_3	−0.4 ± 0.8	1.7 ± 0.1	−0.02 ± 0.00	−1.03 ± 0.00	15	29.0 ± 0.4	1.9 ± 0.1	1.27 ± 0.02	0.26 ± 0.02	23
D_4	−9.9 ± 2.1	1.2 ± 0.1	−0.27 ± 0.00	−1.28 ± 0.00	14	–	–	–	–	–
$D_{1,2}$	−27.9 ± 2.8	1.2 ± 0.2	−0.77 ± 0.01	−1.79 ± 0.01	17	61.6 ± 2.0	1.5 ± 0.1	2.10 ± 0.16	1.09 ± 0.16	12
$D_{1.3}$	−29.9 ± 2.9	1.4 ± 0.2	−0.94 ± 0.01	−1.95 ± 0.01	16	68.1 ± 1.3	1.8 ± 0.1	2.79 ± 0.12	1.78 ± 0.12	9
$D_{1.4}$	−38.4 ± 2.8	1.2 ± 0.2	−1.03 ± 0.01	−2.05 ± 0.01	14	–	–	–	–	–
$D_{2,3}$	2.8 ± 1.0	1.0 ± 0.0	0.07 ± 0.00	−0.95 ± 0.00	23	44.0 ± 0.8	1.4 ± 0.1	1.42 ± 0.04	0.41 ± 0.04	24
$D_{2,4}$	−14.3 ± 0.8	1.1 ± 0.0	−0.36 ± 0.00	−1.37 ± 0.00	13	–	–	–	–	–
$D_{3,4}$	−24.4 ± 1.3	1.2 ± 0.1	−0.68 ± 0.00	−1.69 ± 0.00	11	–	–	–	–	–
$D_{1,2,3}$	−69.6 ± 6.9	1.3 ± 0.4	−2.09 ± 0.04	−3.10 ± 0.05	17	97.3 ± 2.3	1.0 ± 0.1	2.31 ± 0.30	1.30 ± 0.30	6
$D_{1,2,4}$	−62.0 ± 6.4	0.9 ± 0.2	−1.26 ± 0.02	−2.27 ± 0.02	18	–	–	–	–	–
$D_{1,3,4}$	−72.1 ± 9.2	1.2 ± 0.5	−2.06 ± 0.05	−3.07 ± 0.05	18	–	–	–	–	–
$D_{2,3,4}$	−55.3 ± 4.7	0.8 ± 0.1	−1.03 ± 0.01	−2.05 ± 0.01	15	–	–	–	–	–
$D_{1,2,3,4}$	−106.0 ± 4.8	2.5 ± 1.8	−6.03 ± 0.29	−7.05 ± 0.29	13	–	–	–	–	15

tion (R231W) was introduced in the VSD of KCNQ1 and thus may not reflect the general behavior of the channel. To rule out this possibility, we mutated a residue, L353K, in the gate region at the end of the pore-forming S6 helix. Because this mutation lies far from the VSD, we assumed that it should minimally disturb the VSD function, whereas largely affecting the gate

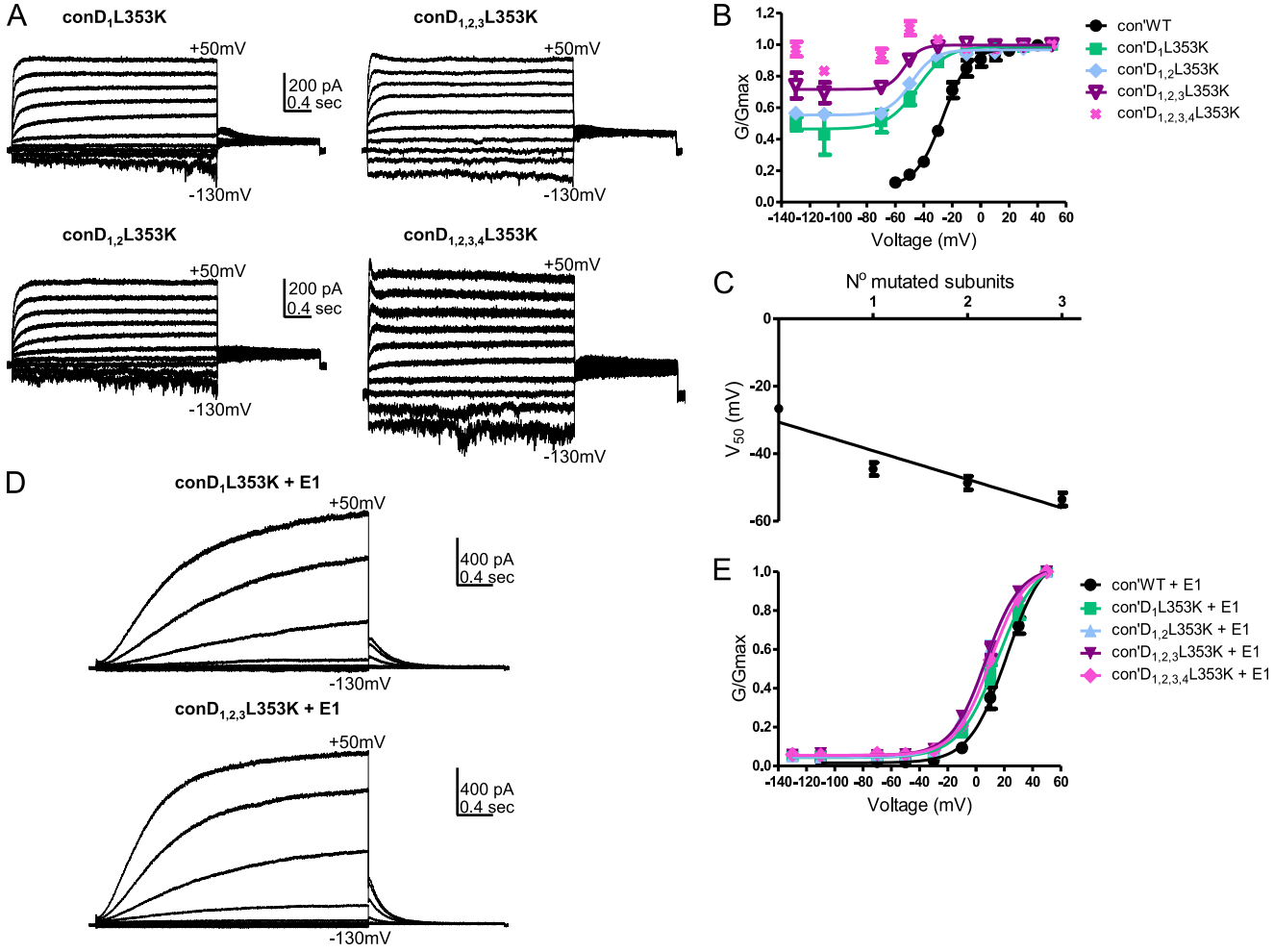

FIGURE 6. **L353K-bearing KCNQ1 subunits produce a gradual left-shift in the voltage dependence of activation.** *A*, representative current traces of Con′, with one, two, three, and four subunits harboring the L353K mutation. The membrane voltage was stepped for 3 s from −130 mV or −110 mV to +50 mV in 20-mV increments and then repolarized for 1.5 s to −60 mV. *B*, conductance-voltage relations of the different R231W-bearing subunits in Con′. Data were fitted with a single Boltzmann function, except for Con′$D_{1,2,3,4}$L353K. Fitting parameters are summarized in Table 3. *C*, linear regression analysis of the different V_{50} values *versus* the number of L353K mutated subunits; $r^2 = 0.87$, $P_v = 0.06$. *D*, representative current traces of Con′D_1L353K and Con′$D_{1,2,3}$L353K, in the presence of KCNE1. *E*, conductance-voltage relations of the different L353K-bearing subunits in Con′ in the presence of KCNE1. Data were fitted with a single Boltzmann function. Fitting parameters are summarized in Table 3.

opening. Interestingly, a proline mutation of this same residue, L353P, was shown to cause a Romano-Ward type of LQT1 syndrome (39). When we sequentially introduced the mutation L353K into an incremental number of subunits, we observed upon KCNQ1 expression alone a progressive left-shift in steady-state activation (V_{50}), which was accompanied by an increased fractional constitutive conductance and constitutive current (WT Con′, $V_{50} = -26.6 \pm 0.8$ mV, $n = 9$; Con′D_1L353K, $V_{50} = -44.5 \pm 1.9$ mV, $n = 6$; Con′$D_{1,2}$L353K, $V_{50} = -48.7 \pm 2.0$ mV, $n = 8$; Con′$D_{1,2,3}$L353K, $V_{50} = -53.5 \pm 2.0$ mV, $n = 9$; Fig. 6, *A* and *B*, Table 3).

Thus, as with the mutant R231W, the gain of function mutant L353K progressively loses its time and voltage dependence with the increasing number of mutated subunits such that it was impossible to determine the V_{50} values in the concatenated constructs bearing four mutated subunits (Fig. 6*A*). Similarly, we found a linear relationship between the V_{50} values and the number of mutated subunits (Fig. 6*C*). Interestingly, the presence of KCNE1 completely abolishes the effect of the mutation (Fig. 6, *D* and *E*, Table 3).

Each KCNQ1 Subunit Endowed with a Loss of Function Mutation Induces an Incremental Gating Perturbation in the Presence of KCNE1—The loss of function mutation, R243W, was introduced at the fourth arginine in the S4 helix, a residue corresponding to R6 in *Shaker* channels. We previously showed in a monomeric KCNQ1 construct that when expressed alone, the mutant R243W expresses functional K^+ currents that appear very similar to those of WT KCNQ1. However, co-expression of R243W with KCNE1 dramatically reduces the currents by producing a right-shift in the voltage dependence of activation (36). The importance of residue Arg-243 for proper channel function is underscored by the existence of naturally occurring long QT mutations (R243C and R243H) leading to profound perturbations in channel gating in the presence of KCNE1 (40, 41). Thus, mutant R243W is very useful for evaluating more specifically the impact of KCNE1 on channel gating because of its silent feature when expressed alone and its perturbing effect in the presence of KCNE1.

When we sequentially introduced in the concatenated tetrameric construct the mutation R243W into an incremental

TABLE 3

Gating parameters of concatenated KCNQ1 and L353K mutant expressed without and with KCNE1

V_{50} (half-activation voltage) and z (equivalent gating charge) were derived by fitting with a single Boltzmann function and are expressed as mean ± S.E. ΔG_0, $\Delta\Delta G_0$, and their standard errors were calculated as described under "Experimental Procedures." –, not detectable.

Subunits mutated	Mutation									
	L353K					L353K + KCNE1				
	V_{50}	z	ΔG_0	$\Delta\Delta G_0$	n	V_{50}	z	ΔG_0	$\Delta\Delta G_0$	n
	mV		*cal/mol*	*kcal/mol*		*mV*		*kcal/mol*	*kcal/mol*	
WT	−26.6 ± 0.8	2.7 ± 0.2	−1.67 ± 0.01		9	25.0 ± 0.6	1.8 ± 0.1	1.01 ± 0.00		14
D_1	−44.5 ± 1.9	2.4 ± 0.4	−2.51 ± 0.03	−0.84 ± 0.03	6	15.5 ± 1.2	1.9 ± 0.1	0.67 ± 0.00	−0.35 ± 0.01	9
$D_{1,2}$	−48.7 ± 2.0	3.2 ± 0.8	−3.54 ± 0.06	−1.86 ± 0.06	8	6.6 ± 0.6	2.1 ± 0.1	0.32 ± 0.00	−0.70 ± 0.00	9
$D_{1,2,3}$	−53.5 ± 2.0	4.6 ± 1.8	−5.72 ± 0.15	−4.05 ± 0.15	9	6.8 ± 0.5	2.1 ± 0.1	0.33 ± 0.00	−0.68 ± 0.00	11
$D_{1,2,3,4}$	–	–	–	–	7	10.3 ± 0.7	2.1 ± 0.1	0.50 ± 0.00	−0.52 ± 0.00	8

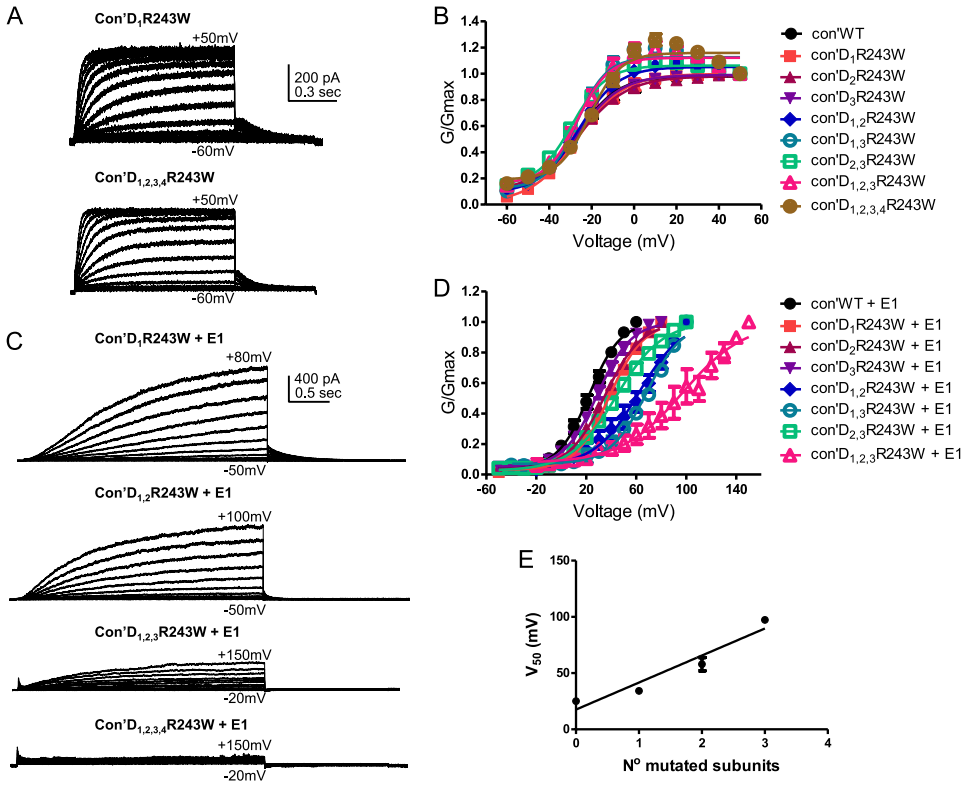

FIGURE 7. **R243W-bearing KCNQ1 subunits produce a gradual right-shift in the voltage dependence of activation.** *A* and *C*, representative current traces of Con′, with the indicated combinations of subunits harboring the R243W mutation in the absence (*A*) or presence (*C*) of KCNE1. CHO cells were held at −90 mV. The membrane voltage was stepped for 1 s (*A*) or 3 s (*B*) from −60 mV to +50 mV in 10-mV increments and then repolarized for 0.5 s to −60 mV. *B* and *D*, conductance-voltage relations of the different combinations of R243W-bearing subunits in Con′ in the absence (*B*) and presence (*D*) of KCNE1. Data were fit with single Boltzmann function. Fitting parameters are summarized in Tables 1 and 2. *E*, linear regression analysis of V_{50} values *versus* the number of R243W mutated subunits in the presence of KCNE1, $r^2 = 0.93$, $P_v = 0.037$.

number of VSDs, we did not observe significant changes in the V_{50} and slope values when compared with WT Con′ in the absence of KCNE1 (Fig. 7, *A* and *B*, Table 1). In contrast, the presence of KCNE1 induced an incremental right-shift of the voltage dependence of channel activation with the increasing number of mutated VSDs (WT Con′+KCNE1, V_{50} = 25.0 ± 0.6 mV, n = 14; Con′D_1R243W+KCNE1, V_{50} = 38.6 ± 0.6 mV, n = 18; Con′$D_{1,2}$R243W+KCNE1, V_{50} = 61.6 ± 2.0 mV, n = 12; Con′$D_{1,2,3}$R243W+KCNE1, V_{50} = 97.3 ± 2.3 mV, n = 6) (Fig. 7, *C* and *D*, Table 2). The right-shift was so large with all four mutated VSDs that we were unable to detect significant currents upon voltage steps larger than +150 mV and thus to determine the corresponding V_{50} value (Fig. 7*C*). We observed a linear relationship between the V_{50} values of the *G-V* curves and the number of mutated subunits (up to three mutated VSDs) again suggesting independence of the VSD motions (Fig. 7*E*). Similar to the gain of function mutation R231W, a positional effect was noticed when considering the V_{50} values between the concatenated constructs bearing two mutated VSDs, with Con′$D_{2,3}$R243W displaying a smaller right-shift when compared with Con′$D_{1,2}$R243W and Con′$D_{1,3}$R243W (Fig. 7*D*).

Thermodynamic Mutant Cycle Analysis of Intersubunit Interactions—Our steady-state electrophysiological data clearly suggest a sequential activation gating scheme for KCNQ1 in both the absence and the presence of KCNE1. The use of thermodynamic mutant cycle analysis can further help to assess the nature of this channel activation process and discriminate between sequential *versus* concerted conformational transitions. For the thermodynamic analysis, the difference in Gibbs

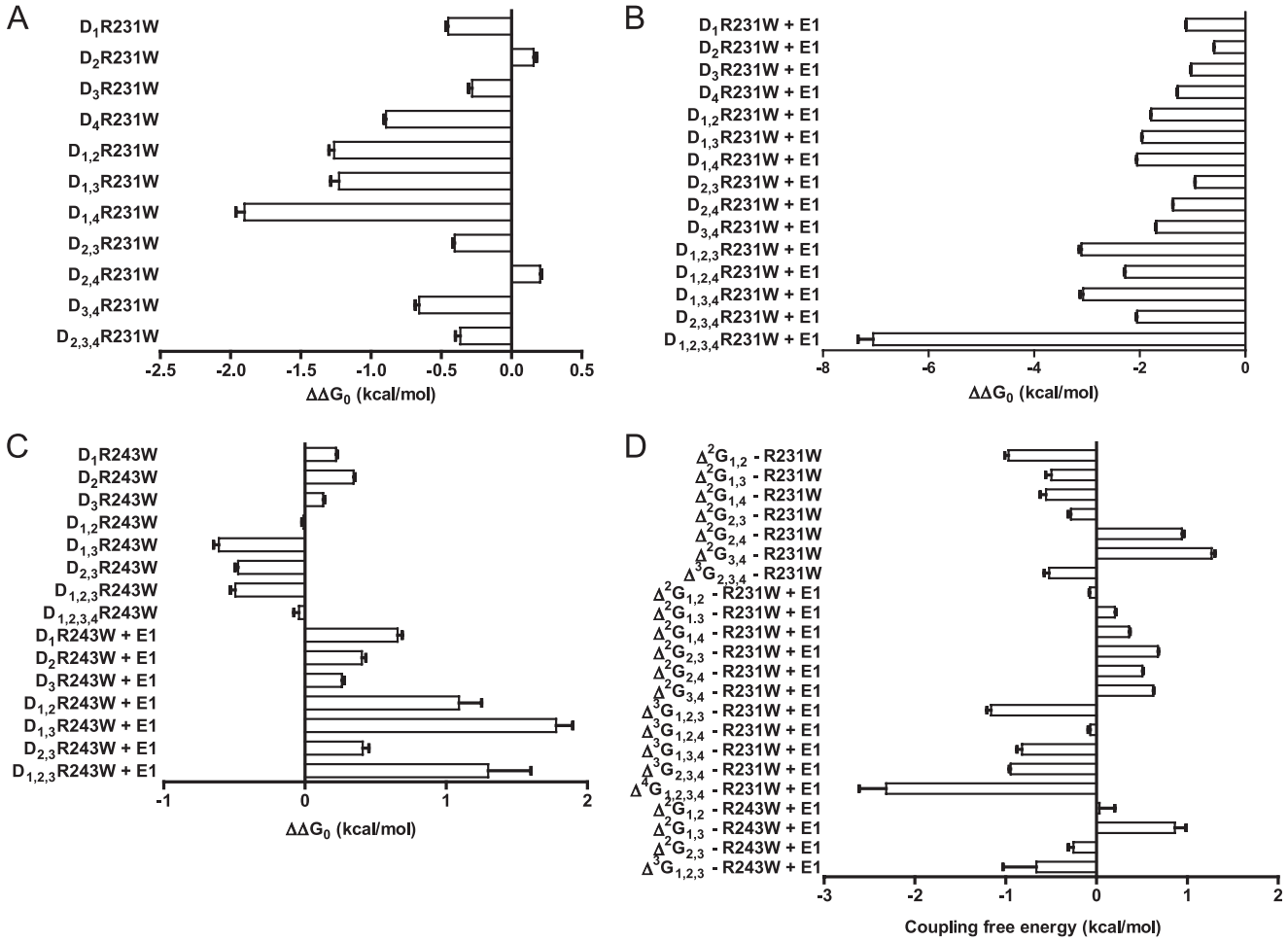

FIGURE 8. **Thermodynamic mutant cycle analysis.** *A* and *B*, the change in free energy difference between the WT and mutants ($\Delta\Delta G_0$ in kcal/mol) was calculated for the Con′ with the different combinations of subunits harboring the R231W mutation in the absence (*A*) and presence of KCNE1 (*B*). *C*, the change in free energy difference between the WT and mutants ($\Delta\Delta G_0$ in kcal/mol) was calculated for the Con′ with the different combinations of subunits harboring the R243W mutation in the absence and presence of KCNE1. *D*, second-, third-, and fourth order coupling free energies (in kcal/mol) between the indicated subunits, calculated as described under "Experimental Procedures."

free energy between the closed and open states (ΔG_0) was calculated, and the change in free energy difference between the WT and mutants ($\Delta\Delta G_0$ in kcal/mol) was deduced (36). For the gain of function mutation R231W, a complete analysis of the Con′R231W expressed alone was not possible because Con′$D_{1,2,3}$R231W and Con′$D_{1,2,3,4}$R231W completely lost their time and voltage dependence, which prevented us from deducing their V_{50} values (Fig. 2). Nevertheless, low $\Delta\Delta G_0$ values were observed with the other concatemer constructs, ranging from 0.16 to 1.9 kcal/mol (Table 1 and Fig. 8*A*). We succeeded in performing a complete thermodynamic mutant cycle analysis for Con′R231W co-expressed with KCNE1, where a gradual increase in $\Delta\Delta G_0$ values was observed with the incremental number of mutated subunits (Fig. 8*B*, Table 2). For Con′D_1R231W+KCNE1, $\Delta\Delta G_0 = -1.12 \pm 0.00$ kcal/mol ($n = 7$); Con′$D_{1,2}$R231W+KCNE1, $\Delta\Delta G_0 = -1.79 \pm 0.01$ kcal/mol ($n = 17$); Con′$D_{1,2,3}$R231W+KCNE1, $\Delta\Delta G_0 = -3.07 \pm 0.04$ kcal/mol ($n = 15$); Con′$D_{1,2,3,4}$R231W+KCNE1, $\Delta\Delta G_0 = -7.05 \pm 0.29$ kcal/mol ($n = 13$) (Fig. 8*B*, Table 2). We calculated the six second-order intersubunit interaction pairs and the four third-order and fourth-order coupling free energies for Con′R231W mutant combinations co-expressed with KCNE1 (Fig. 8*D*, Table 4). Very low values of intersubunit coupling free energies were obtained in all cases, ranging from −0.07 to 2.32 kcal/mol, with the second-order and third-order coupling free energies being lower than that of the fourth-order coupling free energy (Fig. 8*D*, Table 4). For the loss of function mutation R243W in the presence of KCNE1, the same trend was noticed ($\Delta^2G_{1,2} = 0.03 \pm 0.17$ ($n = 12$); $\Delta^3G_{(1,2),3} = -0.66 \pm 0.37$ ($n = 6$)) (Fig. 8, *C* and *D*, Table 4). For Con′$D_{1,2,3,4}$R243W+KCNE1, we could not determine the $\Delta\Delta G_0$ value as the right-shift was so large that we were unable to detect significant currents upon voltage steps above +150 mV, suggesting that the perturbation was very potent. Taken together, these data do not fit with conformational transitions involving large and concerted quaternary rearrangements, but rather imply independence of subunit motions and sequential, weakly cooperative gating transitions.

DISCUSSION

The purpose of this study was to determine the nature of subunit interactions along KCNQ1 activation gating and its modulation by KCNE1, using concatenated tetrameric KCNQ1 channel constructs. Based on a complete thermodynamic mutant cycle

TABLE 4

High-order thermodynamic mutant cycle analysis

Second-and third-order coupling free energies between the indicated subunits were calculated as described under "Experimental Procedures." –, not detectable.

Subunit combination	Mutation[a]		
	R231W	R231W + E1	R243W + E1
		kcal/mol	
$\Delta^2G_{1,2}$	−0.97 ± 0.04	−0.07 ± 0.01	0.03 ± 0.17
$\Delta^2G_{1,3}$	−0.50 ± 0.06	0.20 ± 0.01	0.86 ± 0.12
$\Delta^2G_{1,4}$	−0.56 ± 0.06	0.36 ± 0.01	–
$\Delta^2G_{2,3}$	−0.28 ± 0.03	0.67 ± 0.01	−0.25 ± 0.06
$\Delta^2G_{2,4}$	0.94 ± 0.02	0.50 ± 0.01	–
$\Delta^2G_{3,4}$	1.26 ± 0.04	0.62 ± 0.01	–
$\Delta^3G_{(1,2),3}$	–	−1.16 ± 0.05	−0.66 ± 0.37
$\Delta^3G_{(1,2),4}$	–	−0.07 ± 0.02	–
$\Delta^3G_{(1,3),4}$	–	−0.82 ± 0.06	–
$\Delta^3G_{(2,3),4}$	−0.52 ± 0.05	−0.95 ± 0.02	–
$\Delta^4G_{(1,2)(3,4)}$	–	−2.32 ± 0.30	–

[a] Intersubunit coupling free energies.

analysis of a gain of function mutation, Con′R231W, and a partial analysis of a loss of function mutation, Con′R243W, both co-expressed with KCNE1, our results indicate that contrary to *Shaker* channels, KCNQ1 channels do not experience a late cooperative concerted subunit rearrangement before channel opening. Instead, in both the absence and the presence of KCNE1, KCNQ1 channels undergo sequential, noncooperative gating transitions with independent VSD motions and can open even before all VSDs have moved to an activated conformation.

Independent and cooperative models of voltage sensor movement have been proposed to account for the activation gating of voltage-dependent K^+ channels (20, 22–24, 26, 32, 42). For *Shaker* channels, both steady-state and kinetic studies generally point to sequential and independent motions of the four VSDs contributing to an activated channel closed state, prior to a last concerted and cooperative subunit transition leading to pore opening (20, 22–24, 26). The *Shaker* ILT mutant in S4 has been very instrumental for studying the last transition in the activation pathway because it drastically affects the coupling between gating and channel opening by energetically isolating the activation steps from the cooperative, voltage-independent opening transition (20, 22, 23). Contrasting with the numerous studies performed on *Shaker*-like Kv channels, very little is known about the mechanisms underlying KCNQ1 channel activation and its modulation by the KCNE1 auxiliary subunit. Although gating currents have been recently resolved in KCNQ4 and KCNQ5 channels, no gating current measurements have been reported yet for KCNQ1 channels (43). Interestingly, a voltage clamp fluorometry methodology has been used recently to study the voltage sensor movements upon I_{KS} channel gating (44, 45). As an alternative strategy, we used concatenated tetrameric KCNQ1 channels combined with a thermodynamic mutant cycle analysis to explore the nature of subunit interactions along KCNQ1 gating and its modulation by KCNE1. This approach was valuable for studying cooperative interactions in *Shaker*-like Kv channel gating (19, 27, 32). The similar biophysical properties displayed by the concatenated tetrameric and the monomeric KCNQ1 constructs validated its use to perform a steady-state thermodynamic mutant cycle analysis (Fig. 1).

We first chose a striking gain of function mutation, R231W, at the second arginine in S4 (R2), which was previously shown by us and others to stabilize the channel open state by converting the time- and voltage-dependent K^+ current into a time- and voltage-independent leak K^+ current when expressed as a monomeric mutant construct (35–37). The neutralizing effect of R2 appears to be unique for KCNQ channels because a similar stabilizing open conformation was shown for a mutation at the analogous position in KCNQ2 channels (R201Q) (34). Our data indicate a gradual effect on KCNQ1 gating following sequential introduction of the mutation R231W into an incremental number of VSDs. This effect was reflected by a progressive left-shift of the voltage dependence of channel activation and an increasing instantaneous current (Fig. 2). Unexpectedly, KCNE1 co-expression produced the same incremental effect on channel gating with the increased number of mutated VSDs. Furthermore, a linear relationship between the V_{50} values and the number of mutated subunits was observed, suggesting independence of the VSD motions and lack of significant cooperativity. This feature does not match with a gating model of cooperativity involving concerted conformational transitions of all four VSDs, where it is predicted that the effect of only one mutated VSD on channel gating will be similar to that produced by all four mutated VSDs. Instead, our data are in line with a gating model implying noncooperative, sequential VSD conformational transitions, where a gradual effect on channel gating is expected upon mutation of an incremental number of VSDs.

To assess more directly the effect of KCNE1 on channel gating, we introduced a loss of function mutation, at the fourth arginine in S4, which was previously shown to have a minor impact when expressed alone but to markedly depress the currents when co-expressed with KCNE1 by producing a massive right-shift in the voltage dependence of activation (36). Residue Arg-243 resides at the boundary of the S4 helix and the S4-S5 linker, a critical interface for the functional interaction between KCNQ1 and KCNE1. Previous work suggested that KCNE1 repacks the protein environment around S4, resulting in stark functional consequences in the C-terminal region of S4, which forms crucial protein-protein interactions (37). It was shown that changes in the packing of S4 C terminus by KCNE1 disrupt electrostatic interactions with the conserved glutamate in S2 (Glu-170) and introduce additional steric constraints that make the region less tolerant to tryptophan mutations such as R243W (37). Because mutant R243W unmasks its drastic gating perturbation only in the presence of KCNE1, it was very instrumental for evaluating more specifically the impact of KCNE1 on channel gating. KCNE1 co-expression produced a gradual right-shift in the voltage dependence of channel activation as a result of incremental VSD mutations. Consequently, a linear relationship between the V_{50} values and the number of mutated VSDs was observed, suggesting noncooperative, sequential, and independent VSD motions.

Our data are in line with a recent study using voltage clamp fluorometry to report the voltage sensor movements during KCNQ1 channel gating (45). Similar time course and voltage dependence were found for the fluorescence changes and for conductance activation, suggesting that there is a one-to-one relationship between voltage sensor movement and channel opening, where a single VSD movement leads to gate opening (45). However, in the presence of KCNE1, a wide separation

between the fluorescence-voltage and conductance-voltage curves was measured. In addition, it was found that a voltage sensor movement can occur at large hyperpolarized potentials only in the presence of KCNE1 (45). The data from this recent study thus support the notion that all voltage sensors need to move before the I_{KS} channel can open (45). Although our results do not exclude VSD motions at hyperpolarized potentials, they indicate that KCNE1 co-expression does not change fundamentally the mechanistic process underlying KCNQ1 subunit interactions, implying sequential gating transitions and leading to channel opening even before all VSDs have moved. The complete thermodynamic mutant cycle analysis of Con′R231W and the partial analysis of Con′R243W, both co-expressed with KCNE1, support this view. As clearly illustrated by Zandany *et al.* (27), for a concerted all-or-none transition of channel activation gating, one would expect the second-, third-, and fourth-order coupling free energies to exhibit large and similar values ($\Delta^2G \approx \Delta^3G \approx \Delta^4G$). For Con′R231W+KCNE1, the lack of invariance of the $\Delta\Delta G_0$ values and their gradual increase with the incremental number of mutated subunits discount a concerted cooperative mechanism of subunit interactions. In addition, the very low values of intersubunit coupling free energies and their lack of similarity, with Δ^2G and Δ^3G being lower than Δ^4G, imply a poor intersubunit coupling and render unlikely a gating mechanism involving large, cooperative, and concerted subunit rearrangements. Instead, our data suggest independence of subunit motions and sequential, non-cooperative gating transitions in both the absence and the presence of KCNE1. Furthermore, our data of the gain of function mutant L353K located at the gate region and remote from the VSD confirm the general gating behavior of KCNQ1, which implies an incremental contribution of each subunit to channel opening even before all VSDs have activated.

For each mutation R231W and R243W, a modest positional effect was noticed between the concatenated constructs bearing two mutated VSDs. Several possible reasons may account for this small positional effect. (*a*) The first possibility involves the inherent constraints of the concatenated constructs where the Con′$D_{2,3}$ is the only combination having its N and C termini sandwiched by linkers. Along this line, we previously showed by FRET analysis that the C termini of adjacent KCNQ1 subunits are in proximity and that depolarization brings the C termini of KCNQ1 and KCNE1 close together (46). We also found that the intracellular N and C termini of KCNQ1 also experience a gated motion, which brings them close together (46). In this context and because of the intrinsic constraints of the concatemers, it is possible that the necessary freedom for motions of the intracellular N and C termini of KCNQ1 are restrained in some subunits, notably the Con′$D_{2,3}$, and that the impact of the mutation will slightly differ with the location of the mutated subunit. (*b*) Another possibility is that the nonconcerted and sequential nature of subunit motions may affect the tetrameric symmetry of the channel complex with dissimilar intersubunit interaction energies. For example, the mutated pairs in two diagonally facing subunits (Con′$D_{1,3}$R231W and Con′$D_{2,4}$R231W) have their V_{50} values more depolarized than those of adjacent mutated subunits pairs (Fig. 2*B*, Table 1).

In *Shaker*-like Kv channels, the independent subunit motions are followed by a concerted cooperative mechanism that implies strong intersubunit coupling, which ultimately exerts a force on the S6 lower gate to open. The KCNQ1 gating behavior is very different and may be accounted for by several structural differences with *Shaker* or Kv1.2 channels. In addition to having fewer charges in S4, KCNQ1 lacks the proline in S3 that divides the helix into S3a and S3b, and it has a shorter S3-S4 linker with no negative charges. Although the T1 tetramerization domain of *Shaker*-like channels is located in the N terminus, the KCNQ1 tetramer assembles via its C terminus, which is also endowed with a gating module that binds calmodulin (46–49). In KCNQ1, the post-S6 gating module corresponding to the binding of calmodulin to helix A and B at the proximal C terminus likely plays a crucial role in exerting a sequential strain onto the lower gate to open (47, 48, 50). Our results are in very good agreement with two recently described allosteric gating schemes for KCNQ1 including four horizontal voltage-driven and five vertical voltage-independent transitions (44, 51). Notably, Osteen *et al.* (44), using a very different approach from us, showed by voltage clamp fluorometry that KCNQ1 voltage sensors move relatively independently, but that the channel can conduct before all voltage sensors have activated. This allosteric model provides high flexibility of KCNQ1 upon interaction with accessory subunits, where for example, KCNE1 and KCNE3 subunits will shift the closed-open equilibrium of KCNQ1 toward positive and negative potentials, respectively (51). In this context, our data also indicate that although KCNE1 exerts its well known dramatic impact on KCNQ1 gating by either restricting the VSD motion or/and modifying the coupling between the voltage sensor motion and the opening of the lower gate, it probably does not affect the fundamental mechanisms underlying KCNQ1 subunit interactions, which imply poor intersubunit coupling and nonconcerted sequential gating transitions.

REFERENCES

1. Hernandez, C. C., Zaika, O., Tolstykh, G. P., and Shapiro, M. S. (2008) Regulation of neural KCNQ channels: signaling pathways, structural motifs, and functional implications. *J. Physiol.* **586,** 1811–1821
2. Jentsch, T. J. (2000) Neuronal KCNQ potassium channels: physiology and role in disease. *Nat. Rev. Neurosci.* **1,** 21–30
3. Peroz, D., Rodriguez, N., Choveau, F., Baró, I., Mérot, J., and Loussouarn, G. (2008) Kv7.1 (KCNQ1) properties and channelopathies. *J. Physiol.* **586,** 1785–1789
4. Robbins, J. (2001) KCNQ potassium channels: physiology, pathophysiology, and pharmacology. *Pharmacol. Ther.* **90,** 1–19
5. Abbott, G. W., and Goldstein, S. A. (1998) A superfamily of small potassium channel subunits: form and function of the MinK-related peptides (MiRPs). *Q. Rev. Biophys.* **31,** 357–398
6. Melman, Y. F., Krummerman, A., and McDonald, T. V. (2002) KCNE regulation of KvLQT1 channels: structure-function correlates. *Trends Cardiovasc. Med.* **12,** 182–187
7. Barhanin, J., Lesage, F., Guillemare, E., Fink, M., Lazdunski, M., and Romey, G. (1996) KvLQT1 and lsK (minK) proteins associate to form the I_{KS} cardiac potassium current. *Nature* **384,** 78–80
8. Sanguinetti, M. C., Curran, M. E., Zou, A., Shen, J., Spector, P. S., Atkinson, D. L., and Keating, M. T. (1996) Co-assembly of KvLQT1 and minK (IsK) proteins to form cardiac I_{KS} potassium channel. *Nature* **384,** 80–83
9. Pusch, M., Magrassi, R., Wollnik, B., and Conti, F. (1998) Activation and inactivation of homomeric KvLQT1 potassium channels. *Biophys. J.* **75,** 785–792

10. Tristani-Firouzi, M., and Sanguinetti, M. C. (1998) Voltage-dependent inactivation of the human K^+ channel KvLQT1 is eliminated by association with minimal K^+ channel (minK) subunits. *J. Physiol.* **510,** 37–45
11. Sesti, F., and Goldstein, S. A. (1998) Single-channel characteristics of wild-type I_{KS} channels and channels formed with two minK mutants that cause long QT syndrome. *J. Gen. Physiol.* **112,** 651–663
12. Yang, Y., and Sigworth, F. J. (1998) Single-channel properties of I_{KS} potassium channels. *J. Gen. Physiol.* **112,** 665–678
13. Morin, T. J., and Kobertz, W. R. (2008) Tethering chemistry and K^+ channels. *J. Biol. Chem.* **283,** 25105–25109
14. Wang, K. W., and Goldstein, S. A. (1995) Subunit composition of minK potassium channels. *Neuron* **14,** 1303–1309
15. Nakajo, K., Ulbrich, M. H., Kubo, Y., and Isacoff, E. Y. (2010) Stoichiometry of the KCNQ1-KCNE1 ion channel complex. *Proc. Natl. Acad. Sci. U.S.A.* **107,** 18862–18867
16. Wang, W., Xia, J., and Kass, R. S. (1998) MinK-KvLQT1 fusion proteins, evidence for multiple stoichiometries of the assembled IsK channel. *J. Biol. Chem.* **273,** 34069–34074
17. Long, S. B., Campbell, E. B., and Mackinnon, R. (2005) Crystal structure of a mammalian voltage-dependent Shaker family K^+ channel. *Science* **309,** 897–903
18. Long, S. B., Campbell, E. B., and Mackinnon, R. (2005) Voltage sensor of Kv1.2: structural basis of electromechanical coupling. *Science* **309,** 903–908
19. Gagnon, D. G., and Bezanilla, F. (2009) A single charged voltage sensor is capable of gating the Shaker K^+ channel. *J. Gen. Physiol.* **133,** 467–483
20. Gagnon, D. G., and Bezanilla, F. (2010) The contribution of individual subunits to the coupling of the voltage sensor to pore opening in Shaker K channels: effect of ILT mutations in heterotetramers. *J. Gen. Physiol.* **136,** 555–568
21. Horn, R., Ding, S., and Gruber, H. J. (2000) Immobilizing the moving parts of voltage-gated ion channels. *J. Gen. Physiol.* **116,** 461–476
22. Ledwell, J. L., and Aldrich, R. W. (1999) Mutations in the S4 region isolate the final voltage-dependent cooperative step in potassium channel activation. *J. Gen. Physiol.* **113,** 389–414
23. Pathak, M., Kurtz, L., Tombola, F., and Isacoff, E. (2005) The cooperative voltage sensor motion that gates a potassium channel. *J. Gen. Physiol.* **125,** 57–69
24. Schoppa, N. E., and Sigworth, F. J. (1998) Activation of Shaker potassium channels. III: an activation gating model for wild-type and V2 mutant channels. *J. Gen. Physiol.* **111,** 313–342
25. Yifrach, O., Zandany, N., and Shem-Ad, T. (2009) Examining cooperative gating phenomena in voltage-dependent potassium channels: taking the energetic approach. *Methods Enzymol.* **466,** 179–209
26. Zagotta, W. N., Hoshi, T., and Aldrich, R. W. (1994) Shaker potassium channel gating. III: Evaluation of kinetic models for activation. *J. Gen. Physiol.* **103,** 321–362
27. Zandany, N., Ovadia, M., Orr, I., and Yifrach, O. (2008) Direct analysis of cooperativity in multisubunit allosteric proteins. *Proc. Natl. Acad. Sci. U.S.A.* **105,** 11697–11702
28. Horovitz, A., and Fersht, A. R. (1990) Strategy for analyzing the cooperativity of intramolecular interactions in peptides and proteins. *J. Mol. Biol.* **214,** 613–617
29. Sadovsky, E., and Yifrach, O. (2007) Principles underlying energetic coupling along an allosteric communication trajectory of a voltage-activated K^+ channel. *Proc. Natl. Acad. Sci. U.S.A.* **104,** 19813–19818
30. Isacoff, E. Y., Jan, Y. N., and Jan, L. Y. (1990) Evidence for the formation of heteromultimeric potassium channels in *Xenopus* oocytes. *Nature* **345,** 530–534
31. Kavanaugh, M. P., Hurst, R. S., Yakel, J., Varnum, M. D., Adelman, J. P., and North, R. A. (1992) Multiple subunits of a voltage-dependent potassium channel contribute to the binding site for tetraethylammonium. *Neuron* **8,** 493–497
32. Tytgat, J., and Hess, P. (1992) Evidence for cooperative interactions in potassium channel gating. *Nature* **359,** 420–423
33. Yang, Y., Yan, Y., and Sigworth, F. J. (1997) How does the W434F mutation block current in Shaker potassium channels? *J. Gen. Physiol.* **109,** 779–789
34. Miceli, F., Soldovieri, M. V., Hernandez, C. C., Shapiro, M. S., Annunziato, L., and Taglialatela, M. (2008) Gating consequences of charge neutralization of arginine residues in the S4 segment of Kv7.2, an epilepsy-linked K^+ channel subunit. *Biophys. J.* **95,** 2254–2264
35. Panaghie, G., and Abbott, G. W. (2007) The role of S4 charges in voltage-dependent and voltage-independent KCNQ1 potassium channel complexes. *J. Gen. Physiol.* **129,** 121–133
36. Shamgar, L., Haitin, Y., Yisharel, I., Malka, E., Schottelndreier, H., Peretz, A., Paas, Y., and Attali, B. (2008) KCNE1 constrains the voltage sensor of Kv7.1 K^+ channels. *PLoS ONE* **3,** e1943
37. Wu, D., Pan, H., Delaloye, K., and Cui, J. (2010) KCNE1 remodels the voltage sensor of Kv7.1 to modulate channel function. *Biophys. J.* **99,** 3599–3608
38. Bartos, D. C., Duchatelet, S., Burgess, D. E., Klug, D., Denjoy, I., Peat, R., Lupoglazoff, J. M., Fressart, V., Berthet, M., Ackerman, M. J., January, C. T., Guicheney, P., and Delisle, B. P. (2011) R231C mutation in KCNQ1 causes long QT syndrome type 1 and familial atrial fibrillation. *Heart Rhythm* **8,** 48–55
39. Splawski, I., Shen, J., Timothy, K. W., Vincent, G. M., Lehmann, M. H., and Keating, M. T. (1998) Genomic structure of three long QT syndrome genes: KVLQT1, HERG, and KCNE1. *Genomics* **51,** 86–97
40. Franqueza, L., Lin, M., Shen, J., Splawski, I., Keating, M. T., and Sanguinetti, M. C. (1999) Long QT syndrome-associated mutations in the S4-S5 linker of KvLQT1 potassium channels modify gating and interaction with minK subunits. *J. Biol. Chem.* **274,** 21063–21070
41. Mohammad-Panah, R., Demolombe, S., Neyroud, N., Guicheney, P., Kyndt, F., van den Hoff, M., Baró, I., and Escande, D. (1999) Mutations in a dominant-negative isoform correlate with phenotype in inherited cardiac arrhythmias. *Am. J. Hum. Genet.* **64,** 1015–1023
42. Hodgkin, A. L., and Huxley, A. F. (1952) A quantitative description of membrane current and its application to conduction and excitation in nerve. *J. Physiol.* **117,** 500–544
43. Miceli, F., Cilio, M. R., Taglialatela, M., and Bezanilla, F. (2009) Gating currents from neuronal Kv7.4 channels: general features and correlation with the ionic conductance. *Channels* **3,** 274–283
44. Osteen, J. D., Barro-Soria, R., Robey, S., Sampson, K. J., Kass, R. S., and Larsson, H. P. (2012) Allosteric gating mechanism underlies the flexible gating of KCNQ1 potassium channels. *Proc. Natl. Acad. Sci. U.S.A.* **109,** 7103–7108
45. Osteen, J. D., Gonzalez, C., Sampson, K. J., Iyer, V., Rebolledo, S., Larsson, H. P., and Kass, R. S. (2010) KCNE1 alters the voltage sensor movements necessary to open the KCNQ1 channel gate. *Proc. Natl. Acad. Sci. U.S.A.* **107,** 22710–22715
46. Haitin, Y., Wiener, R., Shaham, D., Peretz, A., Cohen, E. B., Shamgar, L., Pongs, O., Hirsch, J. A., and Attali, B. (2009) Intracellular domains interactions and gated motions of I_{KS} potassium channel subunits. *EMBO J.* **28,** 1994–2005
47. Shamgar, L., Ma, L., Schmitt, N., Haitin, Y., Peretz, A., Wiener, R., Hirsch, J., Pongs, O., and Attali, B. (2006) Calmodulin is essential for cardiac I_{KS} channel gating and assembly: impaired function in long QT mutations. *Circ. Res.* **98,** 1055–1063
48. Wiener, R., Haitin, Y., Shamgar, L., Fernández-Alonso, M. C., Martos, A., Chomsky-Hecht, O., Rivas, G., Attali, B., and Hirsch, J. A. (2008) The KCNQ1 (Kv7.1) COOH terminus, a multitiered scaffold for subunit assembly and protein interaction. *J. Biol. Chem.* **283,** 5815–5830
49. Yellen, G. (2002) The voltage-gated potassium channels and their relatives. *Nature* **419,** 35–42
50. Haitin, Y., and Attali, B. (2008) The C terminus of Kv7 channels: a multifunctional module. *J. Physiol.* **586,** 1803–1810
51. Ma, L. J., Ohmert, I., and Vardanyan, V. (2011) Allosteric features of KCNQ1 gating revealed by alanine scanning mutagenesis. *Biophys. J.* **100,** 885–894
52. Yifrach, O., and MacKinnon, R. (2002) Energetics of pore opening in a voltage-gated K^+ channel. *Cell* **111,** 231–239